

02,13

Josephson tunnel junctions with integral SIN shunting.

© M.S. Shevchenko^{1,2}, L.V. Filippenko¹, O.S. Kiselev^{1,3}, V.P. Koshelets^{1,3}

¹ Kotelnikov Institute of Radio Engineering and Electronics, Russian Academy of Sciences, Moscow, Russia

² Moscow Institute of Physics and Technology (State University), Dolgoprudnyi, Moscow oblast, Russia

³ Institute of Physics of Microstructures, Russian Academy of Sciences, Nizhny Novgorod, Russia

E-mail: shevchenko@hitech.cplire.ru

Received April 29, 2022

Revised April 29, 2022

Accepted May 12, 2022

This work is devoted to the study of tunnel Josephson superconductor-insulator-superconductor (SIS) junctions with a new type of shunting based on the usage of an additional superconductor-insulator-normal metal (NIS) junction located around the SIS junction. Numerical calculations of the parameters of such shunted junctions were carried out and modeling of their IVC (current-voltage characteristics) was performed. The designed samples were manufactured, their parameters were studied. To investigate the behavior of junctions under the influence of high-frequency signals in the sub-THz range, their IVCs were measured.

Keywords: Superconducting devices, superconductor-insulator-superconductor tunnel junction, Josephson effect, shunting of Josephson junctions.

DOI: 10.21883/PSS.2022.09.54154.38HH

1. Introduction

The bypassed Josephson transitions are necessary for the creation of generators and receivers of radiation of THz- and sub-THz-band, superconductor quantum interferometers (SQUIDs), one-quantum digital devices. Bypassing provides a hysteresis-free voltamper characteristic while maintaining a sufficiently high characteristic voltage (and, accordingly, a characteristic frequency) [1]. Typically, thin-film resistors [2,3] are used as bypasses, but this method has drawbacks (large structure size, high parasitic inductance, which reduces the operating frequency of devices) [4]. To address these shortcomings, a new type of bypass was proposed, consisting in the manufacture of tunnel SIS-transitions with integral bypassing by SIN-transition, arranged around the main transition and manufactured with it in the same technological process (Fig. 1). The internal radius of the SIN-transition is determined by the radius of the SIS-transition, the external one is selected taking into account the required resistance. More detailed description of the manufacturing technology and first results can be found in [5].

The new method of bypass SIN- transition allows to significantly reduce the total size of topology and, consequently, to reduce the parasitic inductance of the bypass, which positively affects its operation in the high frequency range. Other ways of internal bypassing are known, which also allow to reduce the size of the structure. There is a way to bypass by manufacturing transitions with a very high current density [2], but with this method it is necessary to produce transitions of a small size (transition

area less than $0.1\mu\text{m}^2$) and with a very thin layer of insulator (order of several atomic layers), such a process is difficult to control. Another method is to manufacture a Josephson transition with a layer of conductive substances, for example, $\text{Nb}_{1-y}\text{Ti}_y\text{N}/\text{Ta}_x\text{N}/\text{Nb}_{1-y}\text{Ti}_y\text{N}$ [6]. The disadvantage of this method of bypassing is the low reproducibility of the required parameters. Studies done [7] show that even samples made on a single substrate vary greatly in the critical currents I_c and normal resistance R_n due to stoichiometry violation.

Thus, the method of integral INS-bypass proposed by us has a number of advantages compared to its analogues. This paper examines the characteristics of such transitions.

2. Simulation

To determine the geometric parameters of transitions with a high characteristic voltage of $V_c = I_c R$ (I_c — critical current of the Josephson transition, R — total bypass resistance and switching voltage below the energy gap) and one-digit VAC (in this case, the McCamper parameter $\beta_c = (2\pi/\Phi_0)I_c R^2 C \lesssim 1$ [1,8], where Φ_0 — quantum magnetic flux, C — junction capacitance) were calculated (Fig. 2). The radius of the bypass ranged from 1.5 to $4\mu\text{m}$. The radius of the shunt ranged from 1.5 to $4\mu\text{m}$.

Fig. 2 shows that in order to achieve a larger characteristic voltage at a lower β_c it is required to produce transitions with high current density (small tunnel resistivity $R_n S$).

In the frame of the numerical simulation, the VAC of the transition with the integral INS bypass (Fig. 3) was also calculated, using the expression for the analytical VAC of

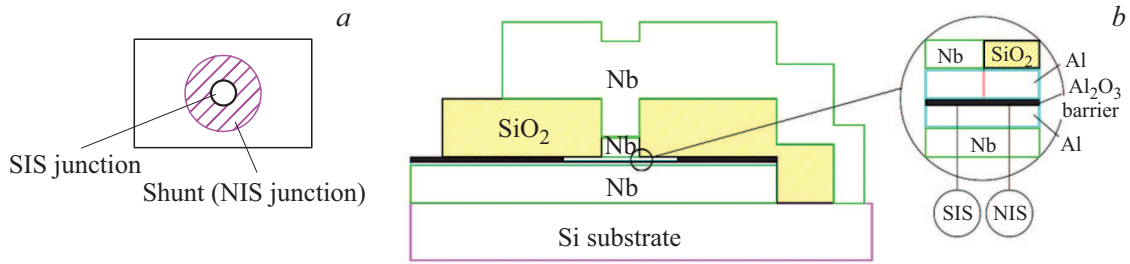


Figure 1. *a* — SIN-transition integral bypassing scheme; *b* — section diagram.

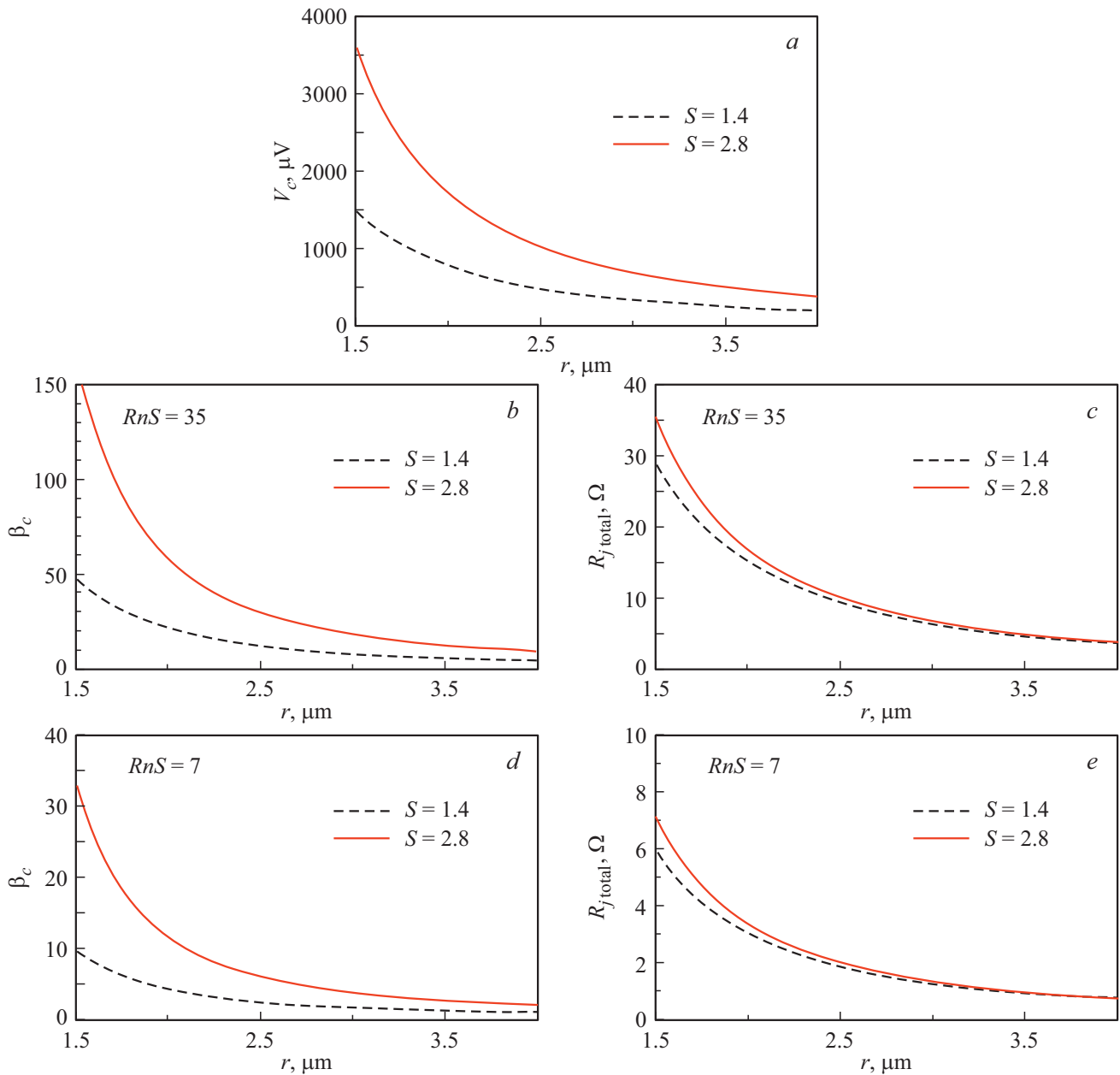


Figure 2. Calculation of parameters of transitions with SIN-bypassing, depending on the outer radius of the bypass and for areas of SIS-1.4 and 2.8 μm^2 . *a* — characteristic voltage V_c ; *b* — hysteresis parameter β_c and *c* — cumulative voltage of bypass and transition $R_{j\text{total}}$ below the energy slit for specific tunnel resistance $RnS = 35 \Omega * \mu\text{m}^2$; *d* — β_c and *e* — $R_{j\text{total}}$ for $RnS = 7 \Omega * \mu\text{m}^2$.

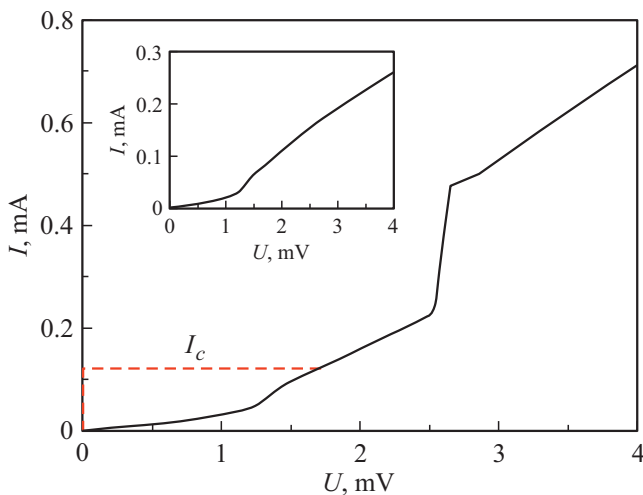


Figure 3. Numerical calculation of a quasi-partial branch of VAC of SIS-transition Nb-Al/AlOx-Nb bypassed by SIN-transition. $T = 4.2$ K. On the inset there is VAC SIN-transition Al-AlOx-Nb with which the bypassing is carried out. Radius of SIS-transition $r_1 = 0.95 \mu\text{m}$; external bypass radius $r_2 = 2 \mu\text{m}$; specific tunnel resistance $R_n S = 30 \Omega * \mu\text{m}^2$; calculated transition parameters with such dimensions and $R_n S$: $V_c = 1300 \mu\text{V}$ and $\beta_c = 30$. The dotted line — the calculated critical current values on the straight branch.

SIN-transition [9]. The developed numerical models allow to determine what parameters will be at transitions with a given current density, geometric dimensions of SIS-transition and bypass; and to determine the necessary parameters for obtaining transitions with the necessary properties.

3. Experimental Studies

The designed samples were manufactured and examined. Fig. 4 shows the experimental VAC of the samples with the integral SIN-bypass for the different external radii of the bypass. You can see that the proposed bypass design really works.

Research was also conducted on the characteristics of bypass structures when they were exposed to a variable signal. The generator used was the distributed Josephson Junction (FFO) [10,11], operating in the range of 300–700 GHz; it was located on the same substrate as the bypass structure. Fig. 5 shows VAC of the bypass transition without signal impact and under the influence of signals of 330, 400 and 460 GHz frequency (at the stresses of $V_n = n\hbar\omega/2e$ the corresponding Shapiro steps are observed, due to the synchronization of the Josephson generation by external signal), and thus we can conclude is that the new type of bypass works at high frequencies as well.

Fig. 6,a shows VAC of the transition with the integral SIN-bypass at different signal power at the frequency 410 GHz. VAC have been measured to derive dependencies of double the critical current amplitude, the amplitude 1st and 2nd Shapiro steps, and the magnitude

estimate of V_c by high-frequency measurements. Step amplitude with the number n provided that the external periodic signal frequency ω is less than or equal to the characteristic frequency of the transition $\omega_c = 2eV_c/\hbar$, is given by the formula $I_n^\pm = I_c J_n(I_\omega/I_c)$ [1], where J_n — Bessel function of the first order, about n , and I_ω — amplitude of external signal.

The first stage amplitude was measured for different frequencies, depending on the power of the generator, which varied due to the change of the current of the FFO at DC voltage (frequency) [10]. Fig. 6, b, c, d shows the dependences of the doubled critical current and the amplitude of the first two current steps on the signal current amplitude I_ω at 410 GHz frequency, which in first approximation is proportional to the root of the superconducting current of PDC at voltage 1 mV [11].

Solid lines and dotted lines show dependencies based on the resistive transition model with a slight attenuation [1,12] — Bessel function of the appropriate order.

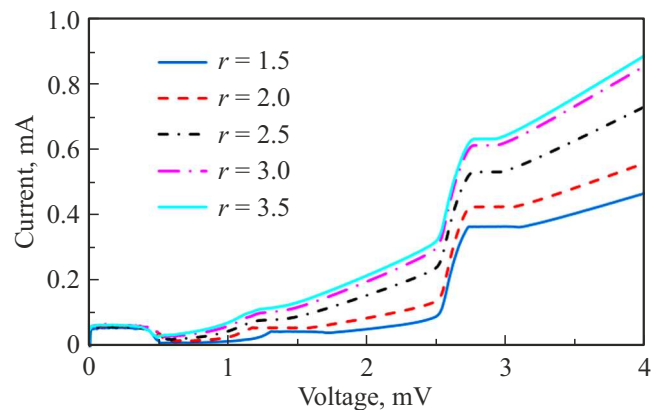


Figure 4. Experimental VAC of transitions with the integral SIN-bypass, measured in voltage setting mode. The SIS-transition area $S = 1.4 \mu\text{m}^2$. The outer radius of the bypass varies from 1.5, μm to 3.5 μm .

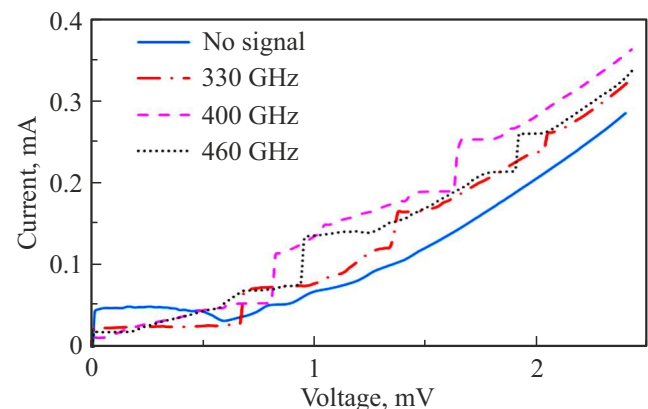


Figure 5. VAC of transitions with the integral SIN-bypass without the influence of the signal and under the influence of signals at the frequency of 330, 400 and 460 GHz. At $V_n = n\hbar\omega/2e$ the Shapiro steps are observed.

These relationships estimate the typical voltage of a bypass transition of V_c^{RF} at high frequency [1]; good convergence of oscillations with an unmodified Bessel function at 410 GHz suggests that the value of V_c^{RF} is of order 0.8 mV.

Measurements of VAC have been made of bypass transitions at different temperatures ranging from 4.2 to 8 K (Fig. 7).

Based on the results of these measurements, the critical current I_c and return current I_r dependences on the voltage value of the energy slit V_g (Fig. 8, a) were plotted. Of the

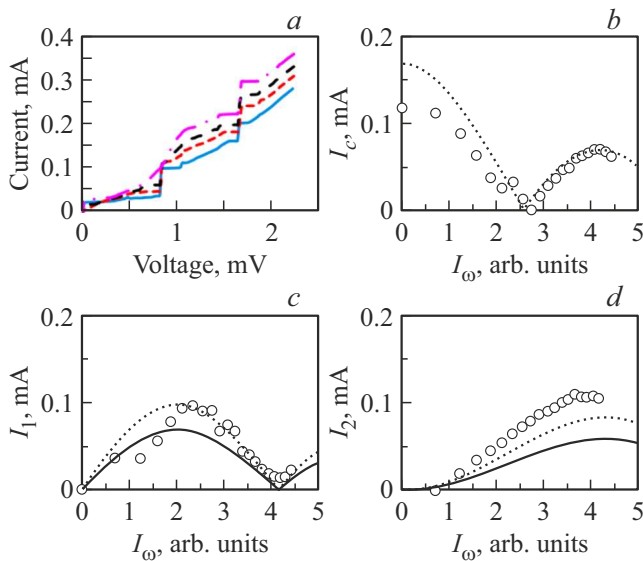


Figure 6. a — VAC of transition with SIN- bypass under the influence of different power FFO signal at 410 GHz; b — double critical current amplitude I_c ; c — amplitude of the first I1 and d — the second I2 Shapiro step depending on the current amplitude of the high-frequency signal I_ω in relative units. Dots — experimental data; dependencies for the resistive model, consistent with the experiment at $I_\omega = 0$, are shown by solid lines; the same dependencies consistent with the experiment at $I_\omega = 4$ are represented by dotted lines.

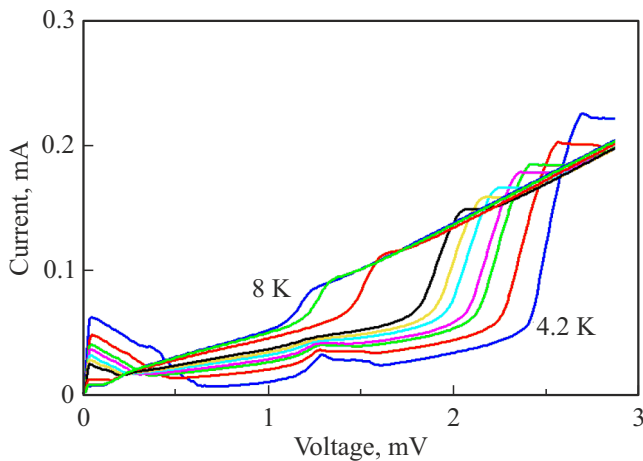


Figure 7. Transition with SIN- bypass at different temperatures ranging from 4.2 K to 8 K. The transition area is $S = 1.4 \mu\text{m}^2$; the outer radius of SIN-transition $r = 1.5, \mu\text{m}$.

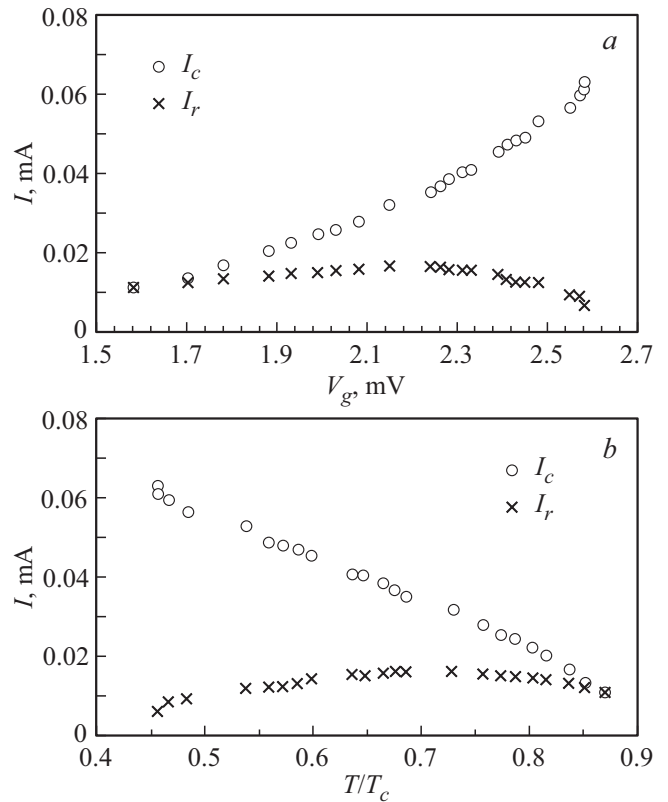


Figure 8. a — Dependence of I_c critical current and return current I_r on energy slit voltage V_g ; b — dependency of critical current I_c and return current I_r on temperature (estimated from V_g). $T_c = 9.2$ K.

value V_g the temperature [13,14] has been estimated, the results are in Fig. 8, b.

Fig. 8 shows that, as predicted in [1], when the critical current decreases, and, respectively, the parameter $\beta_c = (2\pi/\Phi_0)I_c R^2 C$ the ratio I_r/I_c goes to 1, i.e., the VAC of the transition becomes unambiguous. Results presented in Fig. 8, b correspond to the calculations made in [13] within the microscopic theory of superconductivity, taking into account the proximity effect of a volumetric superconductor and a thin film of normal metal for SNINS structures (superconductor-normal metal-insulator-normal metal-superconductor).

4. Conclusion

The design of the transitions was developed with a new integral SIN-bypass. Numerical simulations were carried out and parameters of such transitions were calculated — total bypass and SIS-transition resistance, characteristic voltage, parameter of the McCumber hysteresis. The samples were manufactured, tested by their VAC, as well as behavior under the influence of high-frequency signal. According to the results of studies it can be concluded that the proposed method of bypassing actually functions, including at high

frequencies. The characteristic voltage from high-frequency measurements can be estimated from below by the value of 0.8 mV (frequency 400 GHz). Temperature measurements have also been made that show how the critical transition current changes, and therefore the characteristic voltage depending on the energy slit (temperature).

Funding

This study was financially supported by the Russian Science Foundation (project No. 20-42-04415). Tunnel junctions were prepared under the state assignment of the Kotelnikov Institute of Radio Engineering and Electronics of RAS. For the manufacture of samples, the equipment of UNU No. 352529 Cryointegral was used, the development of which was supported by a grant from the Ministry of Science and Higher Education of the Russian Federation, agreement No. 075-15-2021-667.

Conflict of interest

The authors declare that they have no conflict of interest.

References

- [1] K.K. Likharev. Vvedeniye v dinamiku dzhozefsonovskikh perekhodov (in Russian). Nauka, M. (1985). 320 s. (in Russian).
- [2] S.K. Tolpygo, V. Bolkhovsky, S. Zarr, T.J. Weir, A. Wynn, A.L. Day, L.M. Johnson, M.A. Gouker. *IEEE Transact. Appl. Supercond.* **27**, 4, 1 (2017).
- [3] Tiantian Liang, Guofeng Zhang, Wentao Wu, Yongliang Wang, Lu Zhang, Hua Jin, Xue Zhang, Liliang Ying, Bo Gao. *IEEE Transact. Appl. Supercond.* **30**, 7, 1 (2020).
- [4] C.B. Whan, C.J. Lobb. *J. Appl. Phys.* **77**, 1, 382 (1995).
- [5] M.S. Shevchenko, A.A. Atepalikhin, F.V. Khan, L.V. Filippenko, A.M. Chekushkin, V.P. Koshelets. *IEEE Transact. Appl. Supercond.* **32**, 4, 1 (2021).
- [6] T. Van Duzer, L. Zheng, X. Meng, C. Loyo, S.R. Whiteley, L. Yu, N. Newman, J.M. Rowel, N. Yoshikawa. *Physica C* **372**, 1 (2002).
- [7] Lei Yu, Raghuram Gandikota, Rakesh K. Singh, Lin Gu, David J. Smith, Xiaofan Meng, Xianghui Zeng. *Supercond. Sci. Technol.* **19**, 8, 719 (2006).
- [8] D.E. McCumber. *J. Appl. Phys.* **39**, 3113 (1968).
- [9] D. Chouvaev. Normal metal hot-electron microbolometer with super-conducting Andreev mirrors. Chalmers University of Technology (2001).
- [10] P.N. Dmitriev, L.V. Filippenko, V.P. Koshelets. *Josephson Junctions*. Jenny Stanford Publishing (2017). P. 185–244.
- [11] D.R. Gulevich, V.P. Koshelets, F.V. Kusmartsev. *Phys. Rev. B* **96**, 2, 024515 (2017).
- [12] K.K. Likharev. *Rev. Mod. Phys.* **51**, 1, 101 (1979).
- [13] A.A. Golubov, M.Y. Kupriyanov. *ZhETF* **96**, 1420 (1989) (in Russian).
- [14] A.A. Golubov, E.P. Houwman, J.G. Gijsbertsen, V.M. Krasnov, J. Flokstra, H. Rogalla, M.Y. Kupriyanov. *Phys. Rev. B*, **51**, 2, 1073 (1995).